10.21611/qirt.2016.001

Thickness determination of semitransparent isolated solids using the flash method and an analytical model

by S. J. Altenburg*, H. Weber** and R. Krankenhagen*

* Federal Institute for Materials Research and Testing (BAM), Division 8.7, Unter den Eichen 87, 12205 Berlin, Germany, *Simon.Altenburg@bam.de*

** IBOS Institute for concrete technology and surface protection GmbH, Lennershofstr.162, 44801 Bochum, Germany, *hwe@ibos-labor.eu*

Abstract

As groundwork for thickness determination of polymeric surface protection systems for concrete, we present a method for measuring the thickness of isolated semitransparent solids using pulse thermography both in transmission and reflection geometry. Since standard models [1] do not capture semitransparency, an advanced analytical model by Salazar et al. [2] is applied. Physical material parameters are deduced by fitting experimental data from samples of well-known thickness. Using those, the thickness of samples of the material can be obtained by fitting, as demonstrated for different semitransparent polymer materials.

1. Introduction

So far, no methods of non-destructive thickness determination of surface protection systems for concrete are available. Active thermography is a promising experimental tool for this task. It has the ability to inspect large areas in a reliable and contactless fashion. Usually pulse (or flash) thermography is used for quantitative analysis of defect depth or specimen thickness. Contrary to lock-in thermography, the obtained data contain information about the whole thickness range of the sample in a single measurement, greatly reducing the measurement time. Regarding the thickness determination using pulse thermography, most data analysis methods are primarily aimed at defect depth determination, but some of them can be used for thickness determination as well. The available methods can be divided into two different groups. The peak slope time method (PST) [3], the logarithmic peak second derivative time method (PSDT) [4] and the absolute peak slope time method (APST) [5], e.g., extract a characteristic time from the experimental data, which is related to the defect depth or sample thickness. While PST relies on the thermal contrast to a reference specimen, PSDT and APST do not require a reference. The other approach is fitting of the results of a theoretical model to the experimental data, as proposed by Sun [6, 7]. This method has the advantage of being quite insensitive to noise in the experimental data[1]. Additionally, the complexity of the theoretical model can be adjusted in order to capture the physical effects that most prominently influence the measurements at hand. A comparison of most of these methods is given by Sun [6].

As a first step towards the thickness determination of polymer based surface protection systems for concrete, we examined isolated samples of materials used in such systems. Some of them turned out to be semitransparent in the optical spectral range. Thus, we applied a one-dimensional analytical model based on the work of Salazar et al. [2] to deduce the optical transparency parameters and thermal diffusivities of the respective materials. To evaluate the applicability of the model as a starting point for the development of a model for surface protection systems on concrete, we here use the model for thickness determination of the semitransparent samples using least-square fitting. The model accounts for thermal losses (important for thick samples and materials with low thermal diffusivity) and the specific temporal shape of the heating pulse (important for thin samples and materials with high thermal diffusivity), rendering it applicable to a wide range of materials and sample thicknesses with a single set of physical material parameters. The presented procedure does not depend on a spatially uniform distribution of the heating pulse or the thermal losses (assuming lateral heat conduction can be neglected), which is useful in practical applications. Additionally, the model can be evaluated both in transmission and reflection geometry. Since the model uses physical material parameters, it can directly be used for thickness determination if the thermal diffusivity and the effective optical absorption coefficient in the spectral range of the heat source and the infrared (IR) camera are known. However, since this is usually not the case, these parameters can be obtained from a set of calibration experiments with samples of known thickness. Polymeric samples are specifically difficult for conventional methods: they often are semitransparent and, due to a very small thermal diffusivity, heat losses may play an important role. The model was experimentally verified with samples made from different polymers used in surface protection systems for concrete with thicknesses between $100\,\mu m$ and $2\,mm$. Rather than investigating all aspects and limits of the model, we give an overview.

[1] Note that the aforementioned methods rely on analysis of first or even second derivatives of the measured signal.

2. The analytical model

Here we summarize the utilized analytical model, based on the work by Salazar et al. [2]. While Salazar et al. considered a finite reflectivity of the sample surface and multiple reflections of the incident light beam within the sample, our experimental results have shown that for the investigated samples the effect of multiple reflections is very small and thus was neglected. Multiple reflections within the sample only become important for thin samples of high transparency which have a high reflectivity at the same time. For those very specific samples the more general solution of reference [2] may be applied.

Since the samples used in our experiments were opaque in the spectral range of the used IR camera (see Section 3), the semitransparency in the IR spectrum could be neglected within the considered model as well. The temperature was evaluated at the samples surface for measurements in reflection geometry and at the samples back side for transmission geometry.

The temperature transient calculated by the model depends on the following parameters: the sample thickness L, the optical transparency α, the thermal diffusivity D, the linear heat loss coefficient h, the Laplace transform $\overline{P_0}$ of the normalized temporal shape of the heating pulse P_0, the total energy density Q of the heating pulse[2] and the specific thermal conductivity k. The dependence on k is eliminated by use of normalized parameters $\tilde{h} = h/k$ and $\tilde{Q} = Q/k$. To compare the results of the analytical model to experimental data, the temporal shape of the heating pulse $\overline{P_0}$ has to be known or a suitable approximation has to be chosen. While all other parameters affect the shape of the temperature curve, the intensity parameter Q only affects its amplitude and can therefore be left as a free fitting parameter. Thus, the actually achieved value of energy density during the particular experiment does not have to be determined separately but is a result of data evaluation. Furthermore, it does not need to be spatially homogeneous (as long as lateral heat transfer can be neglected), which is a great benefit in practical applications.

The influence of α and h is illustrated in Fig.1. While the transparency parameter α influences the temperature transient at early times, the effect of a finite heat loss parameter h is observable at later times, as indicated.

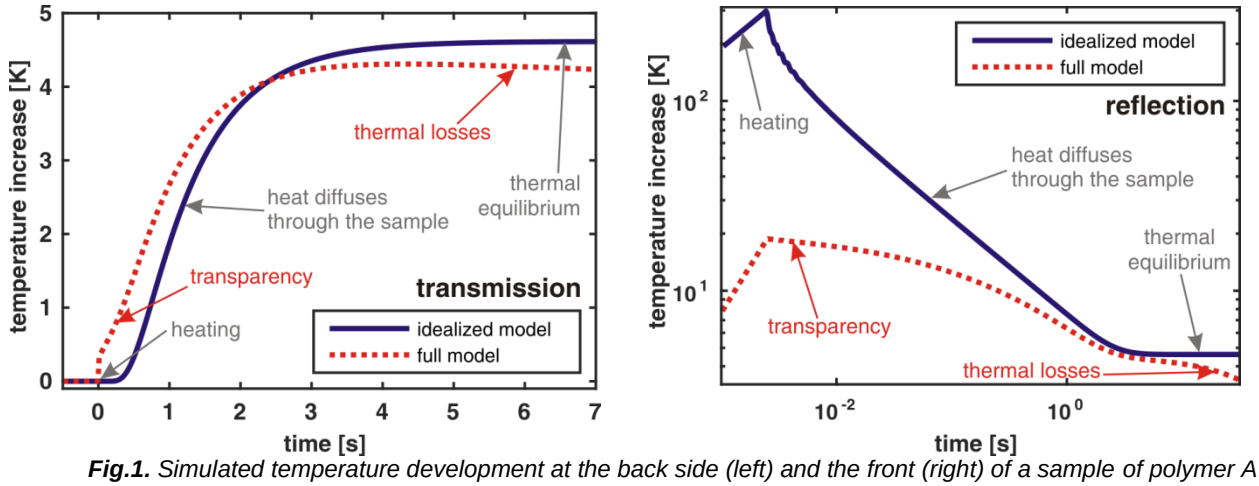

Fig.1. *Simulated temperature development at the back side (left) and the front (right) of a sample of polymer A (see Section 4) of* 1*mm thickness,* $h = 10$*W/m²K,* $Q = 10$*kJ/m²,* $k = 0.2$*W/mK, rectangular heating pulse of* 2.5ms *duration, calculated with (red, dotted line) and without (blue, solid line) semitransparency and heat losses. The different stages of the process are indicated together with the most prominent signatures of semitransparency and heat losses.*

As shown by Salazar et al. [2], the thickness L scales the parameters t (time), D, α and h, influencing the shape of the temperature curve as a whole. An example for temperature curves for one material of different thicknesses is shown in Fig.2. The time $t = 0$s is defined by the start time of the heating pulse.

[2] Note that the term $\overline{P_0}$ includes the energy density Q in reference [2], while here we use a normalized pulse shape $\overline{P_0}$ and a separate energy density Q.

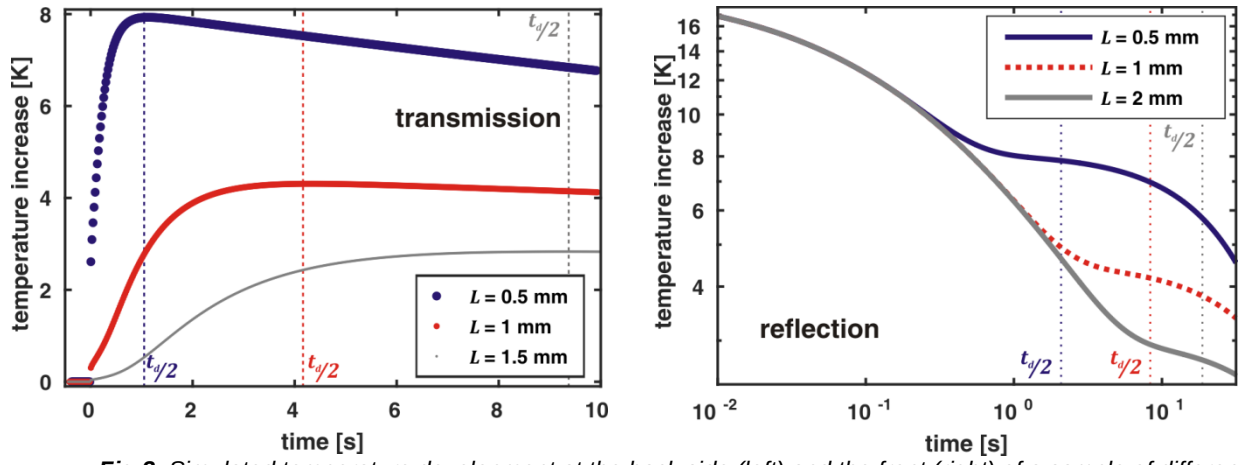

Fig.2. *Simulated temperature development at the back side (left) and the front (right) of a sample of different thicknesses (as indicated) of polymer A (see Section 4, $h = 10 W/m^2K$, $Q = 10 kJ/m^2$, $k = 0.2 W/mK$, Dirac pulse heating). The respective half thermal diffusion times $t_d/2$ are indicated (see text). For times larger than $t_d/2$, the shape of the curves is dominated by the effect of heat losses.*

In order to estimate the necessity for accurate modeling of the temporal shape of the heating pulse, it is useful to compare the duration of the heating pulse τ with the thermal diffusion time $t_d = L^2/D$. If $t_d \gg \tau$ a realistic pulse shape might not be needed, since the system reacts quite slowly on the timescale of the pulse and only the total amount of energy introduced into the system is relevant. In this case the temporal shape of the heating pulse can be described as a Dirac pulse, delivering the total energy density of the pulse instantaneously[3]: $\overline{P_0} = 1$. However, when observing the surface temperature, it cannot be evaluated at times below and close to τ. For laser excitation, the pulse shape may accurately be described by a rectangular pulse of duration τ and $\overline{P_0}(s) = 1 - e_d^{-s\tau}/\tau s$ [2], with s as the Laplace variable. For flash thermography, the heating pulse using a flash lamp is usually very short (order of 1ms) and is often modeled as a Dirac pulse or a rectangular pulse [8]. However, the decay of the flash heating pulse has significant contributions at times well above the time of full width half maximum of the pulse, which has a significant contribution to the temperature development for thin samples and samples with high thermal diffusivity, especially when measuring in reflection geometry. A model describing the temporal shape of the flash excitation pulse more accurately was developed and applied in this work. Details regarding the real pulse shape of flash lamps are beyond the scope of this paper and will be discussed in a forthcoming publication.

As a conclusion, all parameters of the considered analytical model are compiled in Table 1.

Table 1. *Overview of the included physical parameters of the considered analytical model*

Parameter	Meaning	Influence on temperature transient	Calibration	Thickness determination
L	Thickness of the solid	Main parameter for shape and magnitude of the entire transient	Fixed at each position	Fit parameter at each position
D	Thermal Diffusivity	Main parameter for shape of the entire transient	Common fit parameter for each material	Fixed, from calibration
α	Optical absorption coefficient, describes the penetration of the excitation energy into the solid	Short term range	Common fit parameter for each material	Fixed, from calibration
Q	Total energy density introduced by the flash excitation	Scales the entire transient	Fit parameter at each position	Fit parameter at each position
h	(Linear) heat loss coefficient, describes convection as well as radiative thermal losses as a linear approximation	Long term range	Fit parameter at each position	Fit parameter at each position
P_0	Pulse shape parameter, describes temporal shape of the excitation pulse	Short term range	Constant	Constant

[3] The energy density is already accounted for by the parameter Q, the normalization for P_0 is: $\int_{-\infty}^{\infty} P_0(t)dt = 1$.

3. Methods

The experiments were performed using one or two flash lamps with plexiglass as IR filters (model: Hensel Studiotechnik EH Pro 6000, energy consumption up to 6kJ per flash and lamp) and with an IR camera sensitive in the long-wavelength infrared range (model: Infratec ImageIR 8800, NETD: <60mK (30°C), resolution: up to 640×512 pixels, integration time: 140µs). In order to check if the samples were opaque in the cameras spectral range, we performed transmission measurements of selected samples with graphite coating of the side facing the flash lamp, which effectively absorbs its radiation. In this case, the measured temperature transient can only be accurately described by a model disregarding transparency (i.e., $\alpha = \infty$), if the sample is opaque in the spectral range of the camera. This was the case for samples of all the investigated materials. Frame rates up to 1000Hz were used in windowing mode, in order to resolve the temperature development for the thin samples. Typical distances between sample and flash lamps were 30cm, while the distance between camera and sample varied between 80cm and 190cm (larger distances if windowing mode was used in order to increase the framerate).

Five Different polymer materials were investigated, as indicated in table 1. Polymer E (black polyvinylchloride (PVC)) was used as an opaque reference material. For polymers A to D, films of different, non-uniform thickness between 0.1mm and 2mm and with lateral dimensions of about 15cm × 15cm were prepared and suspended in frames made of cardboard. Their thickness was measured at 25 positions each, using an electromagnetic gauge. For polymer E (PVC) a step wedge with thicknesses between 1mm and 4.1mm with similar lateral dimensions was used.

In order to compare the results of the analytical model (based on the Laplace transformation) with experimental data, the inverse Laplace transform has to be applied. In most cases, the algorithm by Stehfest [9, 10] was used to perform this task. Although it is computationally very efficient, it only works well for smooth functions. In some cases, if the temperature shows abrupt changes and the Stehfest algorithm is not applicable, a more computationally expensive but also more accurate algorithm based on the Euler method by Abate and Whitt was used [11].

Fitting was done by minimizing the mean of the squared differences between calculated temperature values and measured temperature values for transmission geometry. For reflection geometry, the mean of the squared differences between the logarithms of the temperature values were minimized, using time dependent logarithmic weight of the data points (i.e., a double logarithmic fit). For all minimization, the simplex search method of Lagarias et al. [12] was used. Differing parameters α_T and α_R were used in transmission and reflection geometry, as discussed in Section 6.

4. Calibration

For calibration, it is advantageous to use measurements of samples of various thicknesses, since the thickness parameter L seemingly influences all other model parameters [2]. A single set of parameters (D, α) should describe the data of samples of different thicknesses. Additionally, the use of a number of data sets for calibration reduces the error resulting from inaccurate reference measurements of the sample thickness and due to nonsystematic external influences on single measurements. Thus, calibration was done by fitting several temperature transients in such a way that a single set of parameters (D, α) was jointly optimized while the energy density Q and the thermal losses h (which might differ depending on the experimental conditions) were individually optimized for each temperature transient (see also Table 1).

For calibration, at least two samples were measured both in reflection and transmission geometry for each material of polymers A to D, resulting in at least 100 temperature curves for calibration. The resulting parameters are listed in Table 2. Regarding the differences between α_T and α_R, see Section 6.

Table 2. *Investigated materials and material parameters from calibration. L_{min} and L_{max} denote the minimum and maximum thicknesses of the respective material used in the experiments*

Abbreviation	Material	L_{min} [mm]	L_{max} [mm]	D [10^{-7}m²/s]	α_T [m^{-1}]	α_R [m^{-1}]
A	StoPox TEP MultiTop	0.9	1.65	1.22	4,550*	5,220
B	MC-DUR 2295	0.21	1.2	1.22	18,600	19,500
C	StoPox WL 100	0.09	1.25	2.23	64,700	127,000
D	StoPox DV 100	0.43	1.7	1.47	11,100	14,100
E	PVC black	1.1	4.1	1.28	100,000*	26,000

* value inaccurate; thinner samples would have been required for a higher sensitivity toward the parameter.

Assuming a value of $k = 0.2$W/mK (PVC, [13]) to convert the reduced fit parameters $\tilde{h}$ and $\tilde{Q}$[4], the values of Q and h usually ranged from 5kJ/m² to 6kJ/m² and from 5W/m²K to 10W/m²K, respectively. Comparing to earlier work using a similar setup [14] the values for the energy density are reasonable. Also the thermal loss parameter h is of a reasonable magnitude [13]. Literature values for the thermal diffusivity for PVC scatter probably due to varying material batches, however, the value of $1.28 \cdot 10^{-7}$m²/s obtained for PVC is close to those previously published [13, 15].

[4] $\tilde{h}$ and $\tilde{Q}$ are not results of the calibration since they remain free fit parameters for thickness determination.

5. Thickness determination

Fig.3 (left) shows reconstructed thicknesses of polymers A to D in dependence of the reference thickness, obtained both in reflection and transmission geometry for 200 fits each. Due to the limited number of available samples (especially for the very small and very large thickness values) 75 of these 400 temperature transients were used both for calibration and evaluation. For thickness determination, the values of D and α from the calibration were used as fixed values, L, h and Q were used as free fit parameters and a realistic pulse shape was applied. The obtained thickness values match the reference values quite well. The right hand side of Fig.3 shows the results of the same calculation without taking into account semitransparency and thermal losses ($h = 0, \alpha = \infty$). While the results are still reasonable, the deviation between determined thickness and reference thickness are larger, especially for small thicknesses (inset) and large thicknesses.

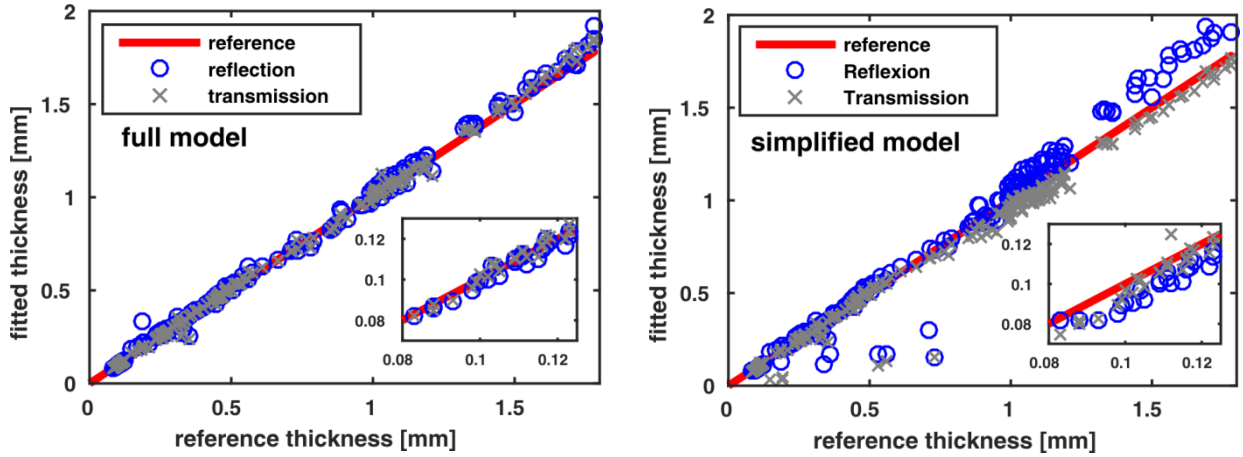

Fig.3. *Determined thicknesses of polymers A to D (200 data points each for transmission and reflection geometry) including semitransparency, realistic pulse shape and thermal losses are shown on the left. The right graph shows the same calculation assuming an opaque sample and absence of thermal losses. As expected, the deviations are larger for the simplified model, especially for large and small thicknesses (insets).*

To analyze systematic differences between determined thickness and reference thickness, the relative differences d are shown in Fig.4. For the full model, there are no clear systematic variations of the relative differences from the reference thickness. Even for the smallest thicknesses the relative differences do not increase. Contrary, for the simplified model and especially for reflection geometry, there are clear systematic deviations from the reference that depend on the particular reference thickness range. For large thicknesses the model tends to yield overestimated values and it yields underestimated values for small thicknesses. All in all, the relative differences spread over a larger range in the simplified model. A quantitative analysis of this data is shown in Table 3.

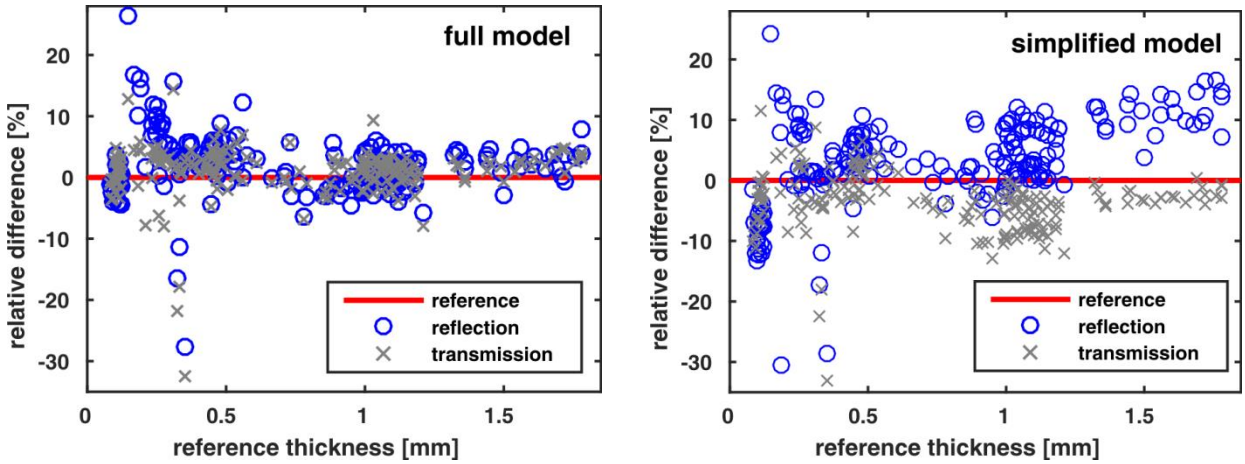

Fig.4. *Relative difference between determined thickness and reference thickness d for data from Fig.3, left: full model, right: simplified model. While there are no clear systematic variations of the relative differences with the reference thickness and most data points are within $\approx \pm 6\%$ for the full model, there are clear systematic deviations from the 0% reference line in the case of the simplified model and the relative differences are spread over a larger range. Note that 12 data points with differences below -35% are not shown in the right graph.*

Table 3. *Mean of the relative differences $\bar{d}$ (measure for a constant systematic error), mean of the absolute relative differences $\overline{|d|}$ (i.e., mean absolute error) and the standard deviation of the relative difference Δd (measure for the scattering of the relative differences) for data from Fig.4. $\overline{|d|}$ and Δd are considerably smaller for the full model in both cases. See also text.*

	Mean relative difference: $\bar{d}$	**Mean absolute relative difference: $\overline{|d|}$**	**Standard deviation of the relative difference: Δd**
Full model, transmission	1.1%	2.9%	4.4%
Full model, reflection	2.3%	4.1%	7.5%
Simplified model, transmission	−5.8%	6.9%	13.7%
Simplified model, reflection	1%	8.2%	14%

The mean of the absolute relative differences $\overline{|d|}$ (i.e., how much the relative difference deviates from the correct value) as well as the standard deviation of the relative differences Δd (i.e., how much the relative differences scatter) are considerably smaller for the full model. The mean of the relative differences $\bar{d}$ (indicating a possible constant systematic deviation) is rather small for the full model. The value of $\bar{d} = -5.8\%$ for the simplified model in transmission geometry indicates an average underestimation of the sample thickness. The small value of $\bar{d}$ for the simplified model in reflection geometry is, however, caused by the different sign of the error for small and large thicknesses (compare Fig.4). All in all, the relative errors of the full model are about half of those of the simplified model and, contrary to the simplified model, do not depend on the sample thickness.

Note that for the calculations of the simplified model only data of times between $0.2\mathrm{t_d}$ and $\mathrm{t_d}$ ($0.2\mathrm{t_d}$ and $2\mathrm{t_d}$) were used in transmission (reflection) geometry, to account for the known deviations between simplified model and experiment. The choice of this time window has a significant influence on the resulting determined thicknesses. Although no systematic study on this issue was performed, the chosen values appeared to yield comparably low relative differences. Using a fixed average value for the thermal losses h may be a viable way to improve the results of the simplified model while reducing the computational effort for the fit. However, a systematic study of this approach is beyond the scope of this work. Using the full model, the used time window is of minor importance, as long as the measurement time was long enough (i.e.,$> t_d$) and the temperature rise was large enough (i.e., larger than about 0.5K at the end of the measurement). The minimum temperature rise is needed to minimize the influence of possible disturbances due to small variations in the surrounding conditions or a small temperature drift of the IR camera.

In order to illustrate the equivalency of the results obtained in the two different experimental setups, Fig.5 shows thickness maps for a sample of polymer B, calculated from both: transmission and reflection experiments. Here, the full model was fitted at each data point of the thermogram (thickness determination). The right part of Fig.5 shows a thermogram of the measurement in reflection geometry.

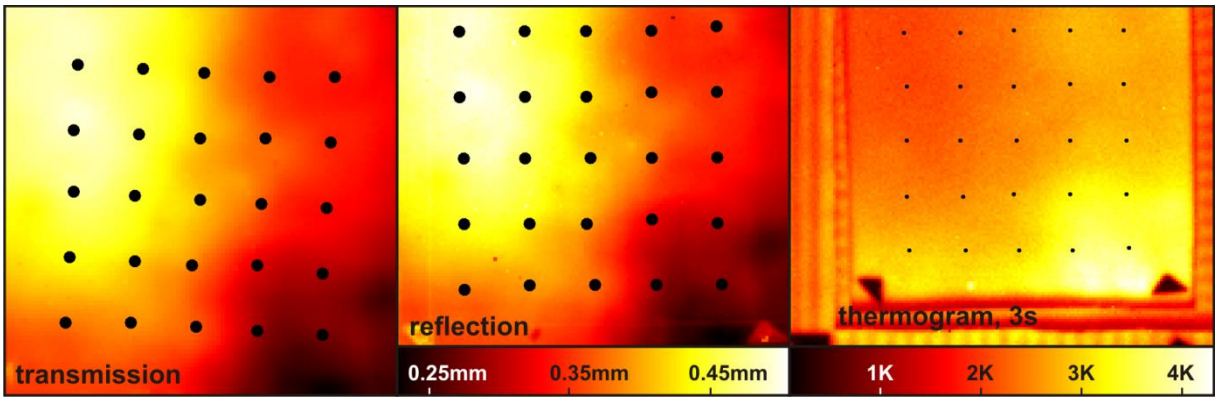

Fig.5. Left and middle: Colorcoded maps (same scale) of thickness of a sample of polymer B, determined by fitting the full model to data of experiments performed in transmission (left) and reflection (middle) geometry for each pixel of the thermogram. The width of the images is ≈ 120 Pixel and ≈ 12cm. The results are very similar. Right: thermogram of the reflection measurement, 3s after flash initiation. Signatures of the cardboard frame and markers for the coordinate system can be observed. The width of the thermogram is ≈ 15cm. Black dots mark positions of reference measurements of the thickness.

6. Transparency

As mentioned above, different values of α were needed in transmission and reflection geometry in order to properly fit the experimental results. Fig.6 shows experimental data and fit results for polymer D obtained in both geometries using the respective transparency parameter. The results of that fit using the other transparency parameter are shown as well and deviate considerably. The origin of this discrepancy is not understood so far. An influence of the

surface structure due to the sample manufacturing was ruled out, since measurements with inverted samples yielded the same results. Thus, the transparency parameter α really depends on the measurement geometry, not the actual orientation of the sample. Additionally to the deviations in the temperature curves, this discrepancy is reflected in the determined thicknesses as well. In this example, in transmission geometry, the thickness of the sample was determined with a deviation of 0.1%, 3.5% and 10% using α_T, α_R and $\alpha = \infty$, respectively. The deviations were even larger in reflection geometry: They were 1%, 10% and more than 30%, respectively. The absorption parameter α_R for reflection geometry is usually larger than α_T for transmission geometry (see Table 2). For the only exception, polymer E, the value of α_T has a very large uncertainty, since the minimum thickness of the sample was too high to show a high sensitivity on the transparency in transmission geometry. Fig.6 also shows the model results assuming a completely opaque material to illustrate the importance of taking the finite semitransparency into account.

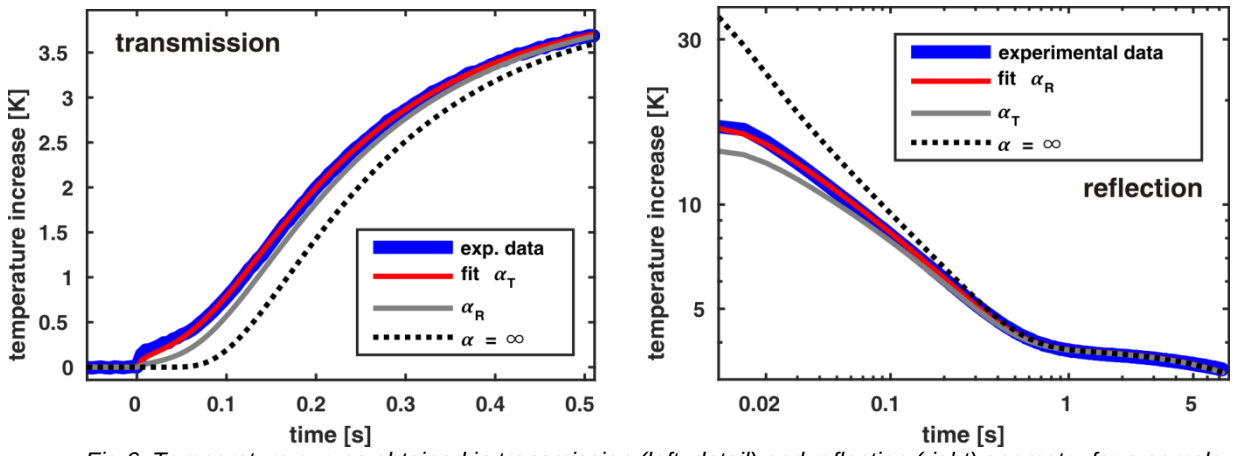

Fig.6. Temperature curves obtained in transmission (left, detail) and reflection (right) geometry for a sample of polymer D of 0.52mm thickness (blue line). A fit using the respective transparency parameter $\alpha_{R/T}$ is shown in red[5], while the result of that fit using other transparency parameters in the model are shown in gray and black (no new fit was performed). There are considerable deviations.

7. Conclusion

We showed that the presented method is suitable for thickness determination of semitransparent isolated solids in both reflection and transmission geometry. It produces good thickness predictions over a large range of sample thicknesses. Especially for thin samples, the relative deviation between determined thickness and reference thickness is much smaller when considering semitransparency and thermal losses than when they are neglected in a simplified model. The method uses physical material parameters which can be obtained by reference measurements. The limits of the model in terms of high transparency of the investigated material, very thin or thick samples or strong spatial variations in the thermal losses are yet to be investigated in detail. We observed a discrepancy between the optical absorption parameter deduced from measurements in transmission and reflection geometry whose origin is also to be studied in future work. However, the results show that the temperature development after optical pulse excitation at typical materials for surface protection of concrete can be accurately described by an analytical model, which will serve as a starting point for thickness determination of these materials on a concrete substrate.

REFERENCES

[1] Parker W. J., Jenkins R. J., Butler C. P., Abbott G. L., Flash method of determining thermal diffusivity, heat capacity, and thermal conductivity, Journal of Applied Physics. - Vol. 32, no 9, pp. 1679-1684, 1961.

[2] Salazar A., Mendioroz A., Apiñaniz E., Pradere C., Noël F., Batsale J.-C., Extending the flash method to measure the thermal diffusivity of semitransparent solids, Measurement Science and Technology. - Vol. 25, no 3, p. 035604, 2014.

[3] Favro L. D., Han X., Kuo P.-K., Thomas R. L., Imaging the early time behavior of reflected thermal wave pulses. 1995. p. 162-166.

[4] Shepard S. M., Lhota J. R., Rubadeux B. A., Wang D., Ahmed T., Reconstruction and enhancement of active thermographic image sequences, Optical Engineering. - Vol. 42, no 5, pp. 1337 - 1342, 2003.

[5] Zeng Z., Zhou J., Tao N., Feng L., Zhang C., Absolute peak slope time based thickness measurement using pulsed thermography, Infrared Physics & Technology. - Vol. 55, no 2–3, pp. 200-204, 2012.

[5] Free fit parameters: L, Q, h

[6] Sun J. G., Analysis of pulsed thermography methods for defect depth prediction, Journal of Heat Transfer. - Vol. 128, no 4, pp. 329-338, 2005.
[7] Sun J., Method for determining defect depth using thermal imaging, patent no. US6542849, 2003.
[8] Balageas D. L., Krapez J. C., Cielo P., Pulsed photothermal modeling of layered materials, Journal of Applied Physics. - Vol. 59, no 2, pp. 348-357, 1986.
[9] Villinger H., Solving cylindrical geothermal problems using the gaver-stehfest inverse laplace transform, GEOPHYSICS. - Vol. 50, no 10, pp. 1581-1587, 1985.
[10] Stehfest H., Algorithm 368 numerical inversion of laplace transforms [d5], Communications of the ACM. - Vol. 13, no 1, pp. 47-49, 1970.
[11] Abate J., Whitt W., A unified framework for numerically inverting laplace transforms, INFORMS Journal on Computing. - Vol. 18, no 4, pp. 408-421, 2006.
[12] Lagarias J. C., Reeds J. A., Wright M. H., Wright P. E., Convergence properties of the nelder-mead simplex method in low dimensions, SIAM Journal on Optimization. - Vol. 9, no 1, pp. 112-147, 1998.
[13] Richter R., Maierhofer C., Kreutzbruck M., Numerical method of active thermography for the reconstruction of back wall geometry, Ndt & E International. - Vol. 54pp. 189-197, 2013.
[14] Krankenhagen R., Maierhofer C., Measurement of the radiative energy output of flash lamps by means of thermal thin probes, Infrared Physics & Technology. - Vol. 67pp. 363 - 370, 2014.
[15] Nunes dos Santos W., Mummery P., Wallwork A., Thermal diffusivity of polymers by the laser flash technique, Polymer Testing. - Vol. 24, no 5, pp. 628-634, 2005.